On Modeling and Tracking Control for a Smart Structure with Stress-dependent Hysteresis Nonlinearity

MA Yan-Hua[1] MAO Jian-Qin[1]

Abstract The performance of smart structures in trajectory tracking under sub-micron level is hindered by the stress-dependent hysteresis generated by varying mechanical loads. In this paper, a stress-dependent Preisach operator is proposed for describing the hysteresis nonlinearity under both varying input current and compressive stress featured by introducing the dependence of the density function on the compressive stress. Subsequently, the properties together with the parameter identification scheme based on a fuzzy tree method of the presented operator are investigated to formulate an inverse compensator. Then, a feedback control scheme combined with a feed-forward compensator is implemented to a magnetostrictive smart structure (MSS) for real-time precise trajectory tracking. Compared with the classical operator, the proposed operator and corresponding control scheme experimentally demonstrate a dramatically improved performance for mitigating the effects of stress-dependent hysteresis.

Key words Stress-dependent hysteresis nonlinearity, Preisach operator, smart structure, tracking control

DOI 10.3724/SP.J.1004.2010.01611

Actuators employing smart materials, such as piezoelectrics, magnetostrictives, electroactive polymers (EAPs), and shape memory alloys (SMAs), have been receiving tremendous interest in the past two decades, due to their broad applications such as micro-vibration control and micro-positioning in the field of aerospace, manufacturing, and defense. Actuators and sensors can be built into structures, often called smart structures, with the ability to sense and respond to environmental changes to achieve desired goals. Fig. 1 illustrates the components of a giant magnetostrictive actuator (GMA). The stroke and output force is provided by the Terfenol-D rod in response to a varying magnetic field generated by the surrounding solenoid coils. A bias magnetic field offered by the permanent magnet and the pre-stress are introduced to produce bidirectional actuation and improve performance of the Terfenol-D rod, respectively.

However, hysteresis, an inherent property of smart materials, restricts their wider application. For the sake of the non-smooth nonlinearity of hysteresis which might cause inaccuracies, oscillations, even instability when the controlled plant exhibits hysteresis behavior[1], modeling, identification as well as control of hysteresis have drawn much attention for its sophisticated nature and extensive applications. In literature, hysteresis is defined through its typical behaviors[2]: 1) memory effect: the output depends on the previous evolution of input; 2) rate-independence: the value of output depends only on the sequence of values reached by the input during the history rather than the "velocity" of the input[3]. The definition is quite effective for the static hysteresis, nevertheless, in real dynamic conditions of technological applications, smart materials are often manipulated under variable mechanical loads motivated by the need for increased levels of adaptability in smart structures, such as in the applications of two-degree high precision tracking platform, as shown in Fig. 1 (b). The compressive stress the GMA suffers, as shown in Figs. 1 (a) and (c), is varying with the deformation of platform structure, which produces measurable changes in the GMA′ hysteretic behavior resulting from the strong coupling between magnetic and mechanical properties of the magnetostrictive rod. That is to say, the output displacement of the GMA depends not only on the input current but also on the compressive stress applied in the longitudinal direction, as shown in Fig. 2, which is defined as stress-dependent hysteresis. Consequently, to combat the typical challenges that restrict the effective use of hysteretic systems, especially in engineering applications, an appropriate purely phenomenological hysteresis model, which is capable of capturing the thorough characteristics of the hysteresis nonlinearities and efficient for real-time control applications, forms the foremost task.

(a) GMA

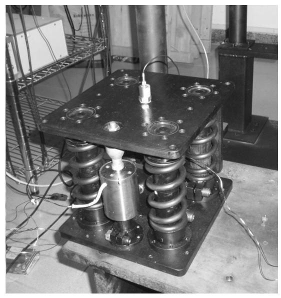

(b) MSS

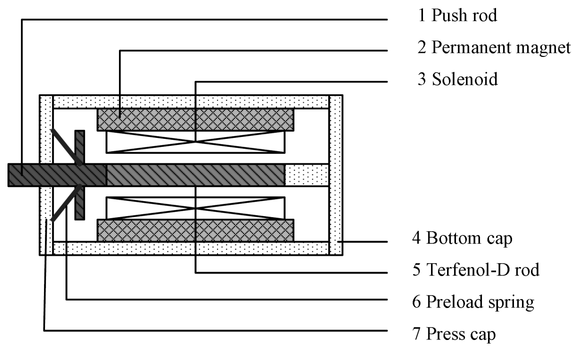

(c) Section view

Fig. 1 GMA and magnetostrictive smart structure (MSS)

Till now, several works have been done on modeling of stress-dependent hysteresis. Bergqvist et al. expanded the classical Preisach operator by treating a compensation of magnetic field and stress as an effective field[4]. Bolshakov

Manuscript received January 20, 2010; accepted August 20, 2010
Supported by the State Key Program of National Natural Science Foundation of China (91016006) and the Specialized Research Fund for the Doctoral Program of Higher Education of China (20070006060)
1. School of Automation Science and Electrical Engineering, Beihang University, Beijing 100191, P. R. China

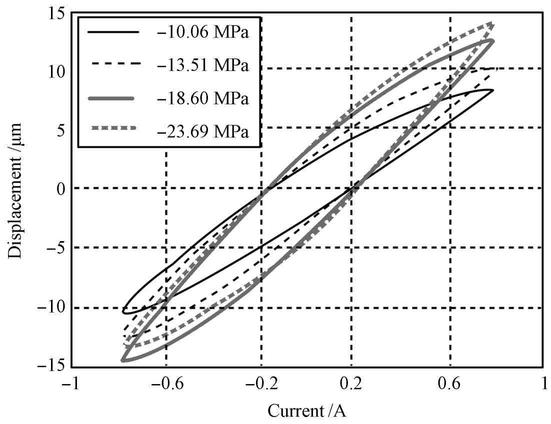

Fig. 2 Stress-dependent hysteresis of a GMA

et al. proposed a new hysteron related to stress[5]. Suzuki et al. addressed a stress-dependent model with the moving Preisach model[6]. Besides, Cavallo et al. described the stress-dependent hysteresis by a stress-dependent density function of classical Preisach operator[7]. Valadkhan et al. developed a new hysteron based on modeling the Gibbs energy for each dipole and the equilibrium states[8]. Zheng et al. proposed a stress-dependent hysteresis model on the basis of Jiles-Atherton model and the theory of magnetomechanical effects and the magnetic force model[9]. However, little work has been done upon modeling stress-dependent hysteresis for the smart structures experiencing varying forces in real-time applications. Control of smart structures with consideration of hysteresis nonlinearity has also received much attention. The basic idea to handle hysteresis is to formulate an accurate model and eliminate the hysteresis with inverse compensation[10−12]. This issue has been widely discussed by either physics-based models[10] or phenomenological models[11−12]. In additional, some feedback control scheme including adaptive control[13], robust control[14], and optimal control[15] were also adopted in the controller synthesis, whereas few studies reported real-time tracking control with compensation for smart structures in the consideration of stress-dependent hysteresis nonlinearity.

In this paper, we study the modeling and trajectory tracking control of an MSS with stress-dependent hysteresis nonlinearity under both variable input current and mechanical stress. First, a stress-dependent Preisach operator is proposed to describe the stress-dependent hysteresis effect. The stress dependency of hysteresis can be modeled phenomenologically by establishing the relationship between the density function and compressive stress. The parameter identification scheme based on a fuzzy tree method is addressed and the mathematical properties of the operator are developed to guarantee the effectiveness of the compensation algorithm. Then, the compensation algorithm based on the proposed hysteresis model is applied to the MSS to cancel out hysteresis for real-time trajectory tracking control. Experiment is conducted to validate the proposed model and the control scheme. In order to improve the tracking accuracy, a feedback controller is adopted, in addition to the feed-forward compensator. Comparing with the traditional PID controller, the results show that the tracking control performance is greatly improved.

1 Stress-dependent hysteresis model

1.1 Stress-dependent Preisach operator

In this subsection, we propose an extension to the classical Preisach operator to describe the stress-dependent characteristics of magnetostrictive hysteresis. One of the advantages of the Preisach operator, as detailed in [3], is that it is purely phenomenological, which means that it is not necessary to establish the relationship between the modeling parameters and the physical mechanism of the hysteresis. Therefore, the stress-dependent hysteresis could be described with regard only to the experimental observations.

The classical Preisach operator $\Gamma[u,\zeta_0]$ is a weighted superposition of delayed relays and $\gamma_{\beta,\alpha}[\cdot,\cdot]$, which are called hysterons. The Preisach operator is defined as

$$\Gamma[u,\zeta_0](t)=\iint_{\alpha\geq\beta}\mu(\beta,\alpha)\gamma_{\beta,\alpha}[u,\zeta_0(\beta,\alpha)](t)\mathrm{d}\beta\mathrm{d}\alpha \tag{1}$$

where ζ_0 is the initial configuration of all hysterons, (β,α) is a pair of thresholds with $\beta\leq\alpha$, and $\mu(\beta,\alpha)$, a Borel measurable function, is the density function.

The main idea behind the stress-dependent hysteresis model can be initiated by including the dependence of the density function on mechanical load m, which generates the stress on the rod. By replacing the density function, the stress-dependent model $\Xi[\cdot,\cdot,\cdot]$ can be written as

$$\Xi[u,\zeta_0,m](t)=\iint_{\alpha\geq\beta}\mu(\beta,\alpha,m)\gamma_{\beta,\alpha}[u,\zeta_0(\beta,\alpha)](t)\mathrm{d}\beta\mathrm{d}\alpha \tag{2}$$

Practically, for the sake of the great variation of mechanical load, the density function expressed above would be severely influenced on the third variable m. To overcome the drawback, adopting some pre-relationship between the density function and m can introduce more accurate mathematical description of the model. Consequently, the stress-dependent model is proposed as

$$\Xi[u,\zeta_0,m](t)=\iint_{\alpha\geq\beta}\mu(\beta,\alpha,g(m))\gamma_{\beta,\alpha}[u,\zeta_0(\beta,\alpha)](t)\mathrm{d}\beta\mathrm{d}\alpha \tag{3}$$

where $g(m)$, a function of the mechanical load m, is employed to adjust the relationship of the hysteresis under different mechanical stresses. Nevertheless, on account of the dependence of the density function on the unknown quantity $g(m)$, numerical implementations of the model is complicated. If $g(m)$ is so chosen that the amplitude has a small variation, then the power series expansion can be used for density function with respect to $g(m)$ as

$$\mu(\beta,\alpha,g(m))=\mu_0(\beta,\alpha)+g(m)\mu_1(\beta,\alpha)+\cdots \tag{4}$$

By (3) and retaining only the first two terms of the expansions, we arrive at the following model:

$$\Xi[u,\zeta_0,m](t)=\iint_{\alpha\geq\beta}\mu_0(\beta,\alpha)\gamma_{\beta,\alpha}[u,\zeta_0(\beta,\alpha)](t)\mathrm{d}\beta\mathrm{d}\alpha+\iint_{\alpha\geq\beta}g(m)\mu_1(\beta,\alpha)\gamma_{\beta,\alpha}[u,\zeta_0(\beta,\alpha)](t)\mathrm{d}\beta\mathrm{d}\alpha \tag{5}$$

It is clear that in the case of very small load, the above model can be reduced to the corresponding classical hysteresis model under no mechanical load. This means that $\mu_0(\beta,\alpha)$ in (5) should coincide with $\mu(\beta,\alpha)$ of the classical

Preisach operator. Then, (5) can be rewritten as

$$\Xi[u,\zeta_0,m](t) = \tilde{y}(t) + \iint_{\alpha\geq\beta} g(m)\mu_1(\beta,\alpha)\gamma_{\beta,\alpha}[u,\zeta_0(\beta,\alpha)](t)\mathrm{d}\beta\mathrm{d}\alpha \quad (6)$$

where $\tilde{y}(t)$ stands for the classical static components of hysteresis under no mechanical load. The second term in (6) represents the variation under different stresses.

The physical principle of the giant magnetostrictive material is used to convince the validity of the proposed model. The existing theory of ferromagnetism treats magnetoelastic hysteresis as a special case of magnetic hysteresis[16]. It is assumed that a varying mechanical stress assists the magnetic field in overcoming the energetic potential barriers to prevent the irreversible magnetizing processes. As described in the previous work[17], an uniaxial stress acts to some extent like an applied magnetic field operating through the magnetostriction. Therefore, the magnetostriction can be described as a function of magnetization and stress. It is the reason why the second term on the right side of (6) is expressed as the hysteresis caused by the magnetic field generated by stress.

1.2 Properties of the model

The following theorems summarize some properties of the stress-dependent Preisach operator, which offer the necessary conditions for the controller synthesis based on inverse compensation. For the convenience during the proof, we would like to describe the proposed model in the (r,s) coordinates with $r=(\alpha-\beta)/2$ and $s=(\alpha+\beta)/2$:

$$\begin{aligned}
&\Xi[u,\varphi_0,g(m)](t) = \\
&\int_0^{\infty}\int_{-\infty}^{\infty}\omega(r,s,g(m))\gamma_{s-r,s+r}[u,\zeta_{\varphi_0}](t)\mathrm{d}s\mathrm{d}r = \\
&\int_0^{\infty}\int_{-\infty}^{\infty}\omega_0(r,s)\gamma_{s-r,s+r}[u,\zeta_{\varphi_0}](t)\mathrm{d}s\mathrm{d}r + \\
&g(m)\int_0^{\infty}\int_{-\infty}^{\infty}\omega_1(r,s)\gamma_{s-r,s+r}[u,\zeta_{\varphi_0}](t)\mathrm{d}s\mathrm{d}r = \\
&2(\int_0^{\infty}\int_{-\infty}^{\varphi[t](r)}\omega_0(r,s)\mathrm{d}s\mathrm{d}r + \\
&g(m)\int_0^{\infty}\int_{-\infty}^{\varphi[t](r)}\omega_1(r,s)\mathrm{d}s\mathrm{d}r) - \nu_{00}
\end{aligned} \quad (7)$$

where $\omega_0(r,s)$ and $\omega_1(r,s)$ are the density functions expressed in the (r,s) coordinates and ν_{00} is the output corresponding to the positive saturation. A memory curve $\varphi[t]$ at time t is the graph of a function of r, φ_0 gives the initial memory curve and ζ_{φ_0} gives the initial state of each hysteron.

Theorem 1. The set of memory curves Ψ is defined to be the set of continuous functions $\varphi:\mathbf{R}_+\rightarrow\mathbf{R}$. Let input $u\in C[0,T]$ and assume ω_1 is a nonnegative measurable density function. For any fixed $m\in\mathbf{R}_+$ and $\varphi_0\in\Psi$:

1) Piecewise monotonicity: if u is either nondecreasing or nonincreasing on some interval in $[0,T]$, then so is $\Xi[u,\varphi_0,g(m)]$;

2) Order preservation: if $u_1<u_2$ on $[0,T]$, then $\Xi[u_1,\varphi_0,g(m)]<\Xi[u_2,\varphi_0,g(m)]$ on $[0,T]$;

3) Strong continuity: $\Xi[u,\varphi_0,g(m)]:C[0,T]\rightarrow C[0,T]$ is strongly continuous.

Theorem 2 (Lipschitz continuity). If $C_1 = \int_0^{\infty}\sup_{s\in\mathbf{R}}|w_0(r,s)|\mathrm{d}r + \sup_{m\in\mathbf{R}_+}|g(m)|\int_0^{\infty}\sup_{s\in\mathbf{R}}|w_1(r,s)|\times\mathrm{d}r<\infty$ and $C_2=\nu_{02}$, then for any $\varphi_0\in\Psi$ and m, $\Xi[u,\varphi_0,g(m)]$ is Lipschitz continuous on $C[0,T]$ with respect to φ and m with Lipschitz constant $2C_1$ and $2C_2$, respectively, where ν_{02} is the output of difference between the stress-dependent and static models corresponding to the positive saturation. Moreover, for any fixed m, $\Xi[u,\varphi_0,g(m)]$ maps bounded subset of X into bounded subset X, where X equals either $C^{0,a}[0,T]$ with $a\in(0,1]$ or $BV[0,T]$.

The analogical proof of the two theorems can be found in [2].

1.3 Parameter identification

In the proposed hysteresis model, density functions $\mu_0(\beta,\alpha)$, $\mu_1(\beta,\alpha)$, and $g(m)$ should be determined. In this paper, a least squares method is adopted to estimate the density functions. This method sourced from Hoffman et al. for identification of the KP operator[18], and Tan et al. expanded it to the Preisach operator[19]. We improve it for the identification of the stress-dependent Preisach operator. In addition, owing to the complexity of $g(m)$, a fuzzy tree method is employed to identify $g(m)$. A detailed treatment of fuzzy tree method can be found in [20]. The identification procedure is separated into three steps.

Step 1. To identify $\mu_0(\beta,\alpha)$, we drive the controlled plant under no mechanical load with a devised piecewise monotone continuous input sequence $u(t)$. For the sake of the capacity of the driving components, the controlled plant cannot reach its positive or negative saturation state and has to operate within a specific range, which is assumed to be $[u_{\min},u_{\max}]$. Thus, the output generated by the outside hysterons can be considered as a constant, denoted by c. Then, the output of the operator at time instant n is yielded as

$$\hat{y}(n) = c + \sum_{k=1}^{q} v_k\gamma_k[n] \quad (8)$$

where q is the number of the hysterons, v_k is the measure to be identified, $\gamma_k[n]$ and $\hat{y}(n)$ denote the state (+1 or −1) of each hysteron and the calculated output at time n, respectively. Let $A_n=\begin{bmatrix}\gamma_1[1] & \gamma_2[1] & \cdots & \gamma_q[1] & 1\\ \vdots & \vdots & \ddots & \vdots & \vdots\\ \gamma_1[n] & \gamma_2[n] & \cdots & \gamma_q[n] & 1\end{bmatrix}$, $X=\begin{bmatrix} v_1 & v_2 & \cdots & v_q & c\end{bmatrix}^{\mathrm{T}}$, $Y_n=\begin{bmatrix}\hat{y}(1) & \hat{y}(2) & \cdots & \hat{y}(n)\end{bmatrix}^{\mathrm{T}}$. The problem becomes to minimize $\frac{1}{2}\parallel A_nX-Y_n\parallel^2$ at time n subject to $X\geq 0$. The row dimensions of A_n and Y_n increase by one after each sampling, and $\mathrm{rank}(A_n)\leq\min\{n,q\}$. The solution part is composed of two parts: a partial SVD of the matrix $A_n^{\mathrm{T}}A_n$ by Lanczos iteration method and the solution of the constrained minimization problem by a line-search Newton-Raphson algorithm. Then, we can obtain a nonsingular measure by assuming that the former identified measure v_k is distributed uniformly over the corresponding cell in the discrete Preisach plane. The corresponding density function $\mu_0(\beta,\alpha)$ is piecewise uniform, which is suitable for the forthcoming inverse algorithm. Alternative methods can also solve the identification issue[21−22].

Step 2. A serial of hysteresis curves between a devised input sequence $u(t)$ and output $y(t)$ at different mechanical loads $m_1,m_2,\cdots,m_j$ are measured experimentally as in Step 1. Define $\bar{y}(t)=y(t)-\tilde{y}(t)$, which describes the difference between the stress-dependent model and the classical

Preisach operator. Rewrite (6) as

$$\bar{y}(t)=\iint_{\alpha\geq\beta} g(m)\mu_1(\beta,\alpha)\gamma_{\beta,\alpha}[u,\zeta_0(\beta,\alpha)](t)\mathrm{d}\beta\mathrm{d}\alpha \quad (9)$$

As discussed previously, $g(m)$ depicts the amplitude of the variation under different stresses. Besides, since $g(m)$ is independent from the input current, (9) can be written as:

$$\bar{y}(t)=g(m)\iint_{\alpha\geq\beta} \mu_1(\beta,\alpha)\gamma_{\beta,\alpha}[u,\zeta_0(\beta,\alpha)](t)\mathrm{d}\beta\mathrm{d}\alpha \quad (10)$$

Define $\bar{y}_j(t)$ to be the displacement variation according to different m_j mentioned before. Assuming $g(m_1)=1$, we treat $\bar{y}_1(t)=\iint_{\alpha\geq\beta}\mu_1(\beta,\alpha)\gamma_{\beta,\alpha}[u,\zeta_0(\beta,\alpha)](t)\mathrm{d}\beta\mathrm{d}\alpha$ as a new classical hysteresis system whose identified scheme has been described in Step 1 and the density function $\mu_1(\beta,\alpha)$ is acquired.

Step 3. From the experimental data, $g(m_j)$ can be calculated by $(\sum_{n=1}^{N}\bar{y}_j[n]/\bar{y}_1[n])/N, j=1,2,\cdots,M$. According to the discrete calculated $g(m_j)$ and the fuzzy tree method, $g(m)$ can be expressed to describe the amplitude difference of stress-dependent model and classical operator.

1.4 Modeling performance

In this subsection, modeling results are compared with experimental data to reveal the performance of the proposed hysteresis operator under compressive stress from -10.96 MPa ~ -23.69 MPa (corresponding mechanical loads from 0 kg $\sim$ 50 kg). The input signal is a sinusoidal current at 1 Hz constrained to $[-0.85\,\mathrm{A}, +0.85\,\mathrm{A}]$. The level L of the discrete Preisach plane is 20, and $[u_{\min}, u_{\max}]$ during the identification procedure is constrained to $[-1\,\mathrm{A}, +1\,\mathrm{A}]$. For the fuzzy tree identification, the maximum nodes $M=8$ and the width $\alpha=3$.

Fig. 3 indicates the comparison between the stress-dependent hysteresis loops measured by experiments and those simulated based on the identification scheme. It is obvious that the simulation results basically agree with the experimental ones. Table 1 lists the root mean square error (RMSE) of a GMA with Terfenol-D rod diameter 7 mm. The errors are defined as:

$$\mathrm{RMSE}=\frac{\sqrt{\sum\limits_{i=1}^{M}(y_{exp}^i-y_{sim}^i)^2}}{M} \quad (11)$$

where y_{exp} is the experimental data, y_{sim} is the results of modeling, and M is the number of data.

In the case that the variation of both stress and input current are concerned simultaneously, the model also can predict the output displacement in the assumption that the stress varies much more slowly than the input current. A compressive stress ranging from 0 N to 500 N is simulated to apply on a GMA as a linear function of time in 200 s. Then, a period of a 1 Hz sinusoidal current with the amplitude of 0.9 A is applied at different time instants. Fig. 4 verifies how the proposed operator is able to describe the actual output displacement. However, a classical Preisach

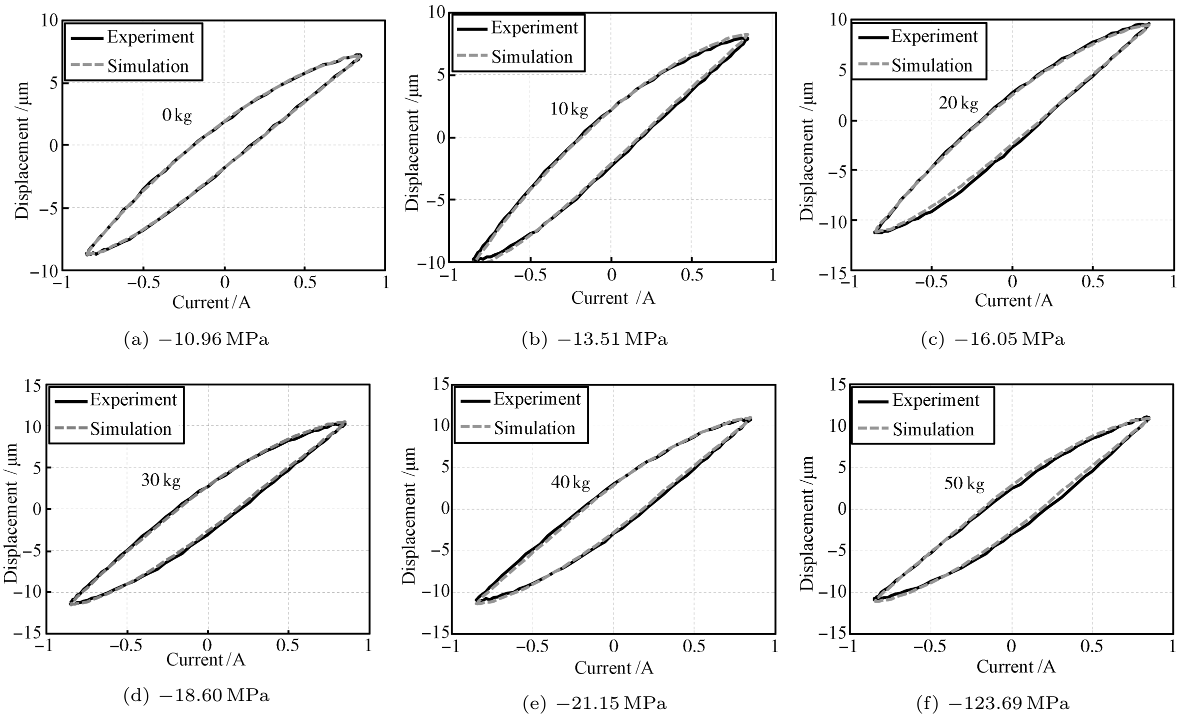

(a) -10.96 MPa (b) -13.51 MPa (c) -16.05 MPa (d) -18.60 MPa (e) -21.15 MPa (f) -123.69 MPa

Fig. 3 Model validation

Table 1 Errors of the proposed stress-dependent models

Load	0 kg	10 kg	20 kg	30 kg	40 kg	50 kg
RMSE	0.0850	0.1495	0.1736	0.1534	0.2103	0.2418

operator identified at the fixed load is incapable to describe the stress-dependent hysteresis of the GMA due to the difference of the hysteresis behaviors of different stresses illustrated in Fig. 2.

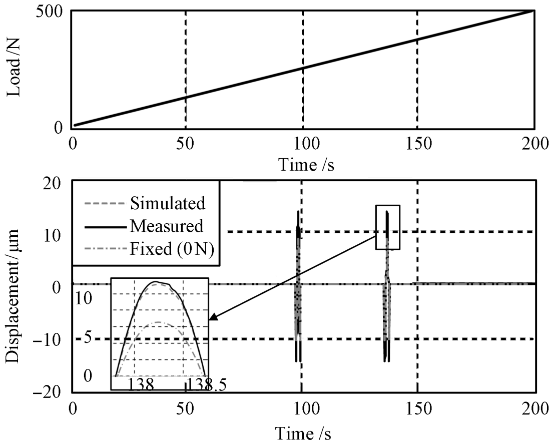

Fig. 4 Modeling of hysteresis (bottom) under slowly varying mechanical load (top) applied in the longitudinal direction of the GMA

2 Trajectory tracking control

An experimental MSS platform was manufactured to achieve 1-DOF trajectory tracking control as shown in Fig. 5. In order to apply the mechanical load in the longitudinal direction, a plate with four linear bearings was designed so that the plate could traverse vertically along the railway, which was fixed into the frame. All of the different mechanical loads were loaded on the plate through the vertical direction of GMA. The top and bottom flexure hinges were employed to prevent the shearing loads. The GMA was manufactured by Beihang University[23], measuring $\Phi 50\,\text{mm} \times 200\,\text{mm}$ with $\Phi 7\,\text{mm} \times 80\,\text{mm}$ Terfenol-D rod, and was driven by GF-20 amplifier operating in current mode, which was controlled by a computer with dSPACE (DS1103) control board. The displacement was measured by an eddy current sensor with a $0.1\,\mu$m resolution. The sampling time was set to 1 ms. It should be noticed that hysteresis of the MSS was also rate-dependent, which meant the hystersis characteristic, being well documented, was related to the excitation rate. In this paper, we only discussed the stress effect on the hysteresis. In order to avoid the effect of the excitation rate, the frequency of input signal was set below 5 Hz for the sake of the rate-independent hysteresis below 5 Hz.

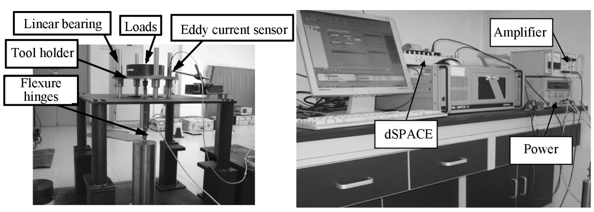

(a) Platform (b) dSPACE control system

Fig. 5 Experiment setup

2.1 Inverse control scheme

A basic idea for controller synthesis for hysteretic system is to predict and linearize the hysteresis nonlinearity by designing a right inverse operator for the hysteresis operator. Fig. 6 shows the block diagram of the tracking control system. However, there are mainly two problems existing in the feed-forward compensator construction of the proposed model. Primarily, we cannot find a closed-form formula for the inverse operator of a Preisach-type model. In addition, since both the input current and the mechanical load are assumed to be the input variables, such an inverse compensator cannot be easily extended from the classical Preisach operator. In this subsection, to overcome the two challenges mentioned before, a compensator based on the strictly increasing property of the proposed hysteresis model is presented with consideration of an assigned mechanical load m from a practical requirement.

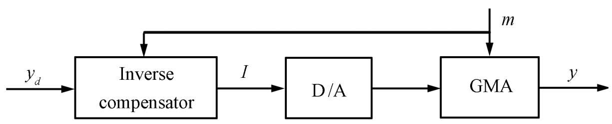

Fig. 6 Diagram of the inverse control scheme

The inverse algorithm was first proposed by Iyer[24], then it was employed into a dynamic hysteresis model[25], and we expanded it for the proposed stress-dependent Preisach operator.

First, we combined the density function of two terms in (4) as the new density function of the proposed hysteresis model:

$$\tilde{\mu}(\beta, \alpha, m) = \mu_0(\beta, \alpha) + g(m)\mu_1(\beta, \alpha) \tag{12}$$

By calculating the value of $g(m)$, the proposed model is reduced to the form of a classical Preisach model by (12) at any prescribed value of the mechanical load. In such conditions, the tracking of a time-varying desired displacement is possible for any constant value of the applied load.

Second, what we have identified in the previous subsection is a set of weighting masses which forms a singular Preisach measure. We can obtain a non-singular Preisach measure by assuming that each identified mass is distributed uniformly over the corresponding cell in the discrete grid. The density function $\tilde{\mu}(\beta, \alpha, m)$ consequently is piecewise uniform, which enables us to solve the inversion problem accurately.

We consider the case of $y > y_0$ and the other case can be treated analogously. It is obvious that $u > u_0$ and we will increase the input in each iteration. At iteration n, let $d_1^n > 0$ such that $u^n + d_1^n$ equals the next input level, and let $d_2^n > 0$ be the minimum amount such that applying $u^n + d_2^n$ will eliminate the next corner of the memory curve. Since the density function is piecewise constant, for $d < \min\{d_1^n, d_2^n\}$, we have

$$\Xi[u^n + d, \phi^n, g(m^*)] - \Xi[u^n, \phi^n, g(m^*)] = a_2^n d^2 + a_1^n d \tag{13}$$

where $a_1, a_2 > 0$ can be computed from $\tilde{\mu}(\beta, \alpha, m)$ and m^* is the fixed load. Let d_0^n such that

$$y - \Xi[u^n, \phi^n, g(m^*)] = a_2^n (d_0^n)^2 + a_1^n (d_0^n)^2 \tag{14}$$

The inversion algorithm now works as follows

$$\begin{cases} d^n = \min\{d_0^n, d_1^n, d_2^n\} \\ u^{n+1} = u^n + d^n \\ y^{n+1} = \Xi[u^{n+1}, \phi^n, g(m^*)] \end{cases} \tag{15}$$

If at iteration n^*, $d^{n^*} = d_0^{n^*}$, then the iteration stops and $u = u^{n^*+1}$.

Finally, an open-loop trajectory tracking control experiment is conducted to test the overall performance of the model and inverse compensation scheme. Fig. 7 illustrates the experimental data of trajectory tracking control with a 2 Hz periodical reference trajectory of 8 μm amplitude under compressive stress of -10.96 MPa (0 kg), -18.60 MPa (30 kg), and -23.69 MPa (50 kg), respectively. It is worthy of noticing that the error shift on the initial stage of tracking control is due to the warm-up of the GMA under compressive stress with a periodical excitation. After running through the warm-up transient stage which lasts less than 0.5 s, the error stops drifting. The experiments confirm that not only the stress-dependent model can basically capture the stress effects of the GMA, but also the scheme of tracking control is effective.

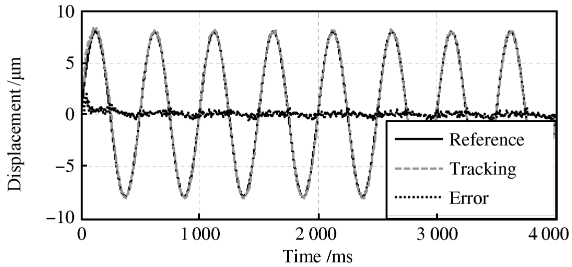

(a) -10.96 MPa with RMSE 0.4778 μm

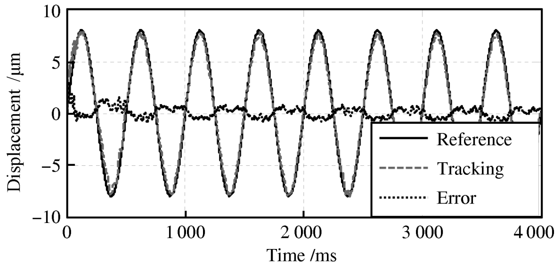

(b) -18.60 MPa with RMSE 1.5072 μm

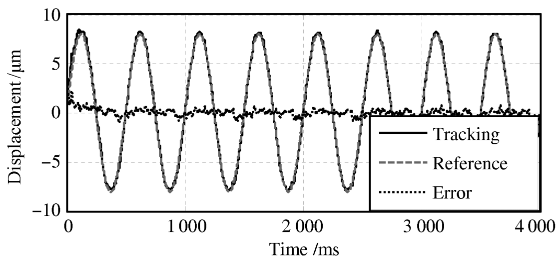

(c) -23.69 MPa with RMSE 0.9108 μm

Fig. 7 Tracking control results of a feed-forward inverse compensator with 2 Hz sinusoid reference trajectory under mechanical load applied in longitudinal direction of GMA

Remark 1. The reference signal should be constrained in the range of the output of the GMA driving between $u_{\min}$ and $u_{\max}$, otherwise the overtopped reference signal may not be attained. To solve the problem, an alternative way is to extend the inputs $u_{\min}$ and $u_{\max}$ during the modeling procedure, or use other predictive methods to estimate the overtopped output.

Remark 2. The former experiments verify the effectiveness of the control strategy as long as the stress is constant, which is the working condition of the experiments. If the stress varies with time, we can calculate $g(m)$ to figure out the variation item on-line similar to Subsection 2.1 on condition that we are sure of the mechanical load m.

Remark 3. The experiment is very susceptive to the initial condition of the GMA because of the demagnetization effect of the Terfenol-D rod, thus we should confirm that the initial conditions of the experiments is consistent with the simulation procedure.

2.2 Combined control scheme

In order to improve the accuracy of tracking control, a PID feedback controller combined with inverse compensation in the feed-forward loop is used for real-time tracking control. Fig. 8 shows the block diagram of the tracking control system. The hysteresis nonlinearity could be eliminated by the hysteresis compensator in the feed-forward loop, and the PID feedback controller is adopted to deal with the remaining nonlinear uncertainties generated by the inverse compensator, the dynamic characteristic of the MSS as well as the disturbance. In the feed-forward loop, the compensator current $I_f(kT)$, corresponding to the desired displacement $x_d(kT)$ is obtained from the feed-forward compensator proposed in Subsection 2.1. In the feedback loop, the desired displacement is compared with the measured displacement of the MSS, and the error signal is sent to a PID controller to compute the additional control output current ΔI. This control signal is added to the feed-forward control current and then sent to the GMA. The control output for this controller is

$$u(k) = K_p e(k) + K_p \frac{T}{T_I} \sum e(k) + K_p \frac{T_D}{T}[e(k) - e(k-1)] + I_f(k) \tag{16}$$

where T denotes the sampling time interval.

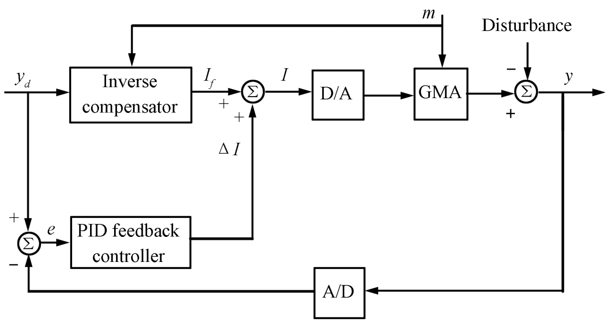

Fig. 8 Diagram of the combined control scheme

Fig. 9 reports the trajectory tracking control results of the combined control scheme. To further compare the tracking performance, tests using a 2 Hz periodical reference signal with an amplitude of 8 μm under -18.60 MPa (30 kg) compressive stress were performed between the regular PID feedback control and the PID control with a feed-forward loop. It is evident from Fig. 10 that significant improvement of tracking accuracy is achieved for a PID controller with a feed-forward loop.

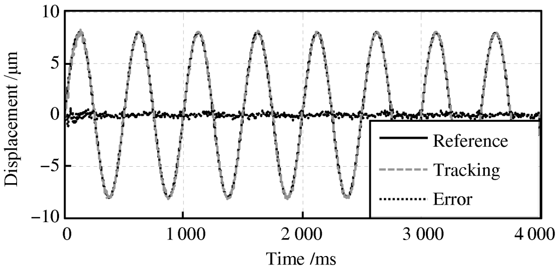

(a) −10.96 MPa with RMSE 0.2589 μm

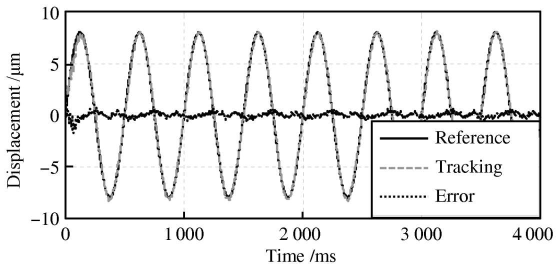

(b) −18.60 MPa with RMSE 0.7609 μm

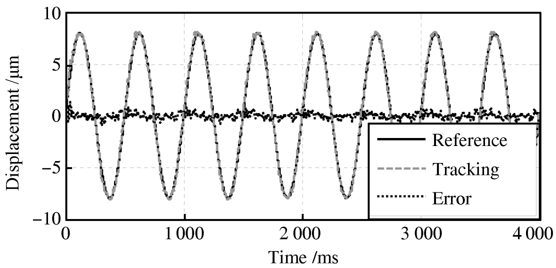

(c) −23.69 MPa with RMSE 0.4244 μm

Fig. 9 Tracking control results of a PID controller incorporated with a feed-forward inverse compensator with 2 Hz sinusoid reference trajectory under mechanical load applied in the longitudinal direction of the GMA

The proposed control scheme also can be applied to a 2-DOF magnetostrictive module, as shown in Fig. 1 (b), to eliminate the stress-dependent hysteresis aiming at 2-DOF micro-positioning. The schematic view of the module is illustrated in Fig. 11, which consists of two GMAs placed orthogonally to generate vertical and horizontal displacements and forces as well as a decoupled control action in the two translational directions, and four spring-rubber elements for passive support and damper. The vertical GMA joints the top module with the base via two flexible joints in each end, in order that the output force of the GMA is going through directly the axis of the Terfonol-D rod. A flexible joint is employed to connect the output pole of the horizontal GMA and the module, whereas the bottom of the horizontal GMA is fixed directly to the base. The spring-rubber element is settled to the base through the adjustment fixture. If the load varies, the adjustment fixture can be regulated to change compression degree of the spring and alter the height of the module. Then, the position of the vertical GMA will be adjusted by another adjustment fixture such that the gravity of the load on the work platform will be only carried by the four spring-rubber elements, and the inertial force of the load on the work platform will be carried by the GMA and the spring-rubber elements. The GMAs measure $\Phi\,50\,\text{mm} \times 64\,\text{mm}$ with $\Phi\,10\,\text{mm} \times 40\,\text{mm}$ Terfenol-D rod. The mechanical load is applied in the vertical direction. By the combined control scheme presented in this subsection, a trajectory tracking control in both directions with an amplitude of 5 μm 1 Hz sine wave under −16.05 MPa (20 kg) compressive stress was performed. Simulation results as shown in Fig. 12 verify the proposed control scheme.

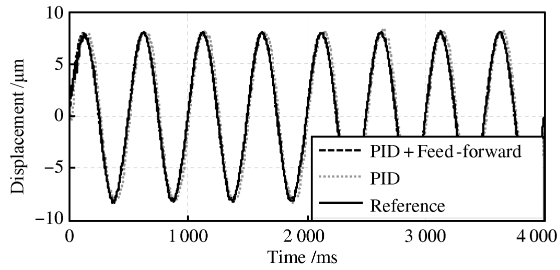

(a) Trajectories of reference signal, output displacement of a PID controller and a combined controller

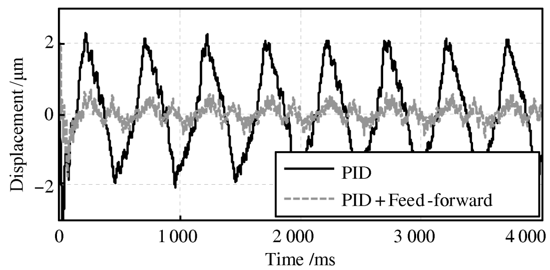

(b) Error of the PID control scheme with RMSE 1.8669 μm and the combined control scheme with RMSE 0.7609 μm

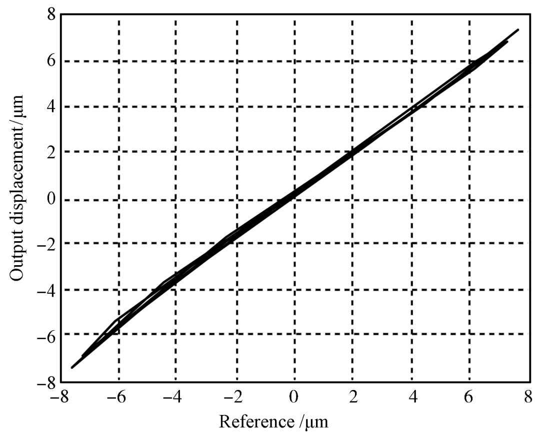

(c) Output displacement only with inverse feedforward compensator

Fig. 10 Comparison of tracking results between a regular PID controller and a PID controller combined with inverse compensation in the feedforward loop with a 2 Hz sinusoid reference signal under −18.60 MPa compressive stress

Remark 4. Hysteresis, especially a stress-dependent hysteresis, is a class of complex nonlinearity, which indicates that a pure linear controller cannot eliminate the error causing by it. The reason why a PID controller, a typical linear controller, is adopted for the system is that most hysteresis nonlinearity has been canceled by the feed-forward compensator, and only a small amount as well as other disturbance is left to be dealt with by the feedback linear controller, as shown in Fig. 10 (c). Experimental results confirm that the hysteresis property existing in the smart materials and structures is a class of strong nonlinearity and could not be easily dealt with by a linear controller.

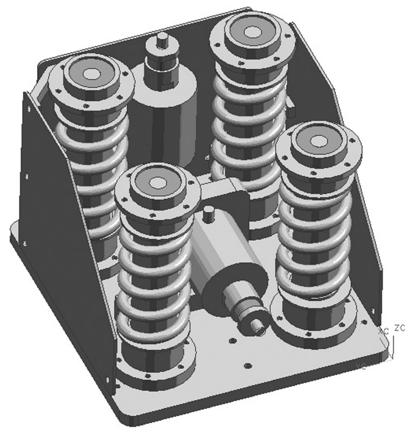

Fig. 11 Schematic view of the magnetostrictive module

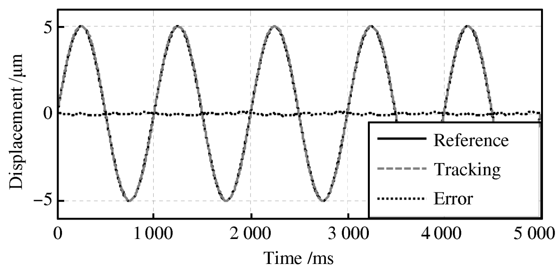

(a) Vertical direction with RMSE 0.1008 μm

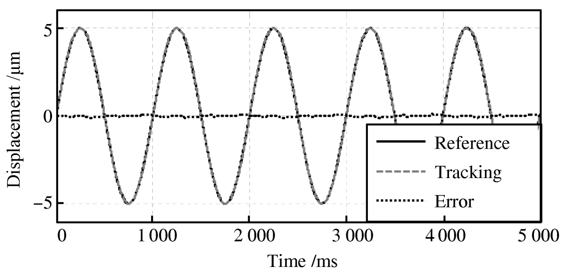

(b) Horizontal direction with RMSE 0.1697 μm

Fig. 12 Tracking control results with a PID controller incorporated with stress-dependent hysteresis compensation in the feed-forward loop

Remark 5. Because the model which we derived to describe the hysteresis nonlinearity is a numerical model and an analytical form is not available, the control parameters cannot be directly computed. Also other theoretical parameter tuning methods are not suitable for a system that incorporate the feed-forward loop. Thus, the trial and error method was used to determine the control parameters.

3 Discussions

It is worthwhile to notice that the proposed modeling and tracking control scheme is not only for the MSS mentioned in the paper, but also available for the smart structures which exhibit the characteristic of stress-dependent hysteresis. Moreover, by adopting the dynamic model of the smart structures, both stress-dependent and rate-dependent phenomena could be described and the corresponding controller synthesis could also be achieved.

The performance of experiments is quite sensitive to model uncertainties, errors introduced by the inverse schemes as well as the experiment disturbance due to the open loop nature of the feed-forward. Even though the adoption of a PID feedback controller could eliminate the errors of the compensator, the contradiction between the stability and precision of the whole system during the tuning period could not be ignored. To solve this problem, we can consider the inverse error and experiment disturbance as an external disturbance and attenuate it by robust or other control techniques.

Compressive stress ranging from -10.96 MPa to -23.69 MPa is included in the modeling experiments in this paper. The proposed model is still valid for a wider range of compressive stress through the experimental data. In addition, advanced predictive technique would do a lot of favor in prediction and interpolation of $g(m)$ to improve the accuracy of both modeling and control results.

4 Conclusion

The main contribution of this paper is to propose a systematic approach for applications of a hysteresis nonlinear model to precise tracking control of an MSS. We model the hysteresis by the improved stress-dependent Preisach operator. In addition, the mathematical properties as well as the method for parameter identification has also been provided. Based on the model, an inverse control scheme together with a feedback controller combining a feed-forward compensator has been developed. Experimental results demonstrate that the operator can capture stress-dependent hysteretic effects, and that our identification and control schemes are effective.

Acknowledgement

The first author would like to sincerely thank Professor Li Lin and Doctor Yang Yong for their provision of the experiment equipment.

References

1 Tao G, Kokotovic P V. Adaptive control of plants with unknown hystereses. *IEEE Transactions on Automatic Control*, 1995, **40**(2): 200−212

2 Visintin A. *Differential Models of Hysteresis*. New York: Springer-Verlag, 1994. 12−14

3 Mayergoyz I D. *Mathematical Models of Hysteresis and Their Applications*. New York: Elsevier, 2003. 108−116

4 Bergqvist A, Engdahl G. A stress-dependent magnetic Preisach hysteresis model. *IEEE Transactions on Magnetics*, 1991, **27**(6): 4796−4798

5 Bolshakov G V, Lapovok A J. A Preisach model for magnetoelastic hysteresis. *Journal of Magnetism and Magnetic Materials*, 1996, **162**(1): 112−116

6 Suzuki T, Matsumoto E. Comparison of Jiles-Atherton and Preisach models extended to stress dependence in magnetoelastic behaviors of a ferromagnetic material. *Journal of Materials Processing Technology*, 2005, **161**(1-2): 141−145

7 Cavallo A, Davino D, de Maria G, Natale C, Pirozzi S, Visone C. Hysteresis compensation of smart actuators under variable stress conditions. *Physica B: Condensed Matter*, 2008, **403**(2-3): 261−265

8 Valadkhan S, Shum A, Morris K A. Load-dependent hysteresis of magnetostrictive materials. In: Proceedings of the Conference on Modeling, Signal Processing, and Control for Smart Structures. San Diego, USA: SPIE, 2007. 652316: 1−10

9 Zheng J J, Cao S Y, Wang H L. Modeling of magnetomechanical effect behaviors in a giant magnetostrictive device under compressive stress. *Sensors and Actuators A: Physical*, 2008, **143**(2): 207−214

10 Smith R C. Inverse compensation for hysteresis in magnetostrictive transducers. *Mathematical and Computer Modelling*, 2001, **33**(1-3): 285−298

11 Zhang X L, Tan Y H, Su M Y, Xie Y Q. Neural networks based identification and compensation of rate-dependent hysteresis in piezoelectric actuators. *Physica B: Condensed Matter*, 2010, **405**(12): 2687−2693

12 Mokaberi B, Requicha A A G. Compensation of scanner creep and hysteresis for AFM nanomanipulation. *IEEE Transactions on Automation Science and Engineering*, 2008, **5**(2): 197−206

13 Chen X K, Hisayama T, Su C Y. Pseudo-inverse-based adaptive control for uncertain discrete time systems preceded by hysteresis. *Automatica*, 2009, **45**(2): 469−476

14 Feng Y, Rabbath C A, Hong H, Al Janaideh M, Su C Y. Robust control for shape memory alloy micro-actuators based flap positioning system. In: Proceedings of the American Control Conference. Baltimore, USA: IEEE, 2010. 4181−4186

15 Oates W S, Smith R C. Nonlinear optimal control techniques for vibration attenuation using magnetostrictive actuators. *Journal of Intelligent Material Systems and Structures*, 2008, **19**(2): 193−209

16 Vonsovskii S V, Shour Y S. *Ferromagnetism*. Moscow: State Technical and Theoretical Press, 1948. 83−91

17 Dapino M J, Smith R C, Flatau A B. Structural magnetic strain model for magnetostrictive transducers. *IEEE Transactions on Magnetics*, 2000, **36**(3): 545−556

18 Hoffman K H, Meyer G H. A least squares method for finding the Preisach hysteresis operator from measurements. *Numerische Mathematic*, 1989, **55**(6): 695−710

19 Tan X B, Venkataraman R, Krishnaprasad P S. Control of hysteresis: theory and experimental results. In: Proceedings of the Conference on Modeling, Signal Processing, and Control in Smart Structures and Materials. Bellingham, USA: SPIE, 2004. 101−112

20 Mao J Q, Zhang J G, Yue Y F, Ding H S. Adaptive-tree-structure-based fuzzy inference system. *IEEE Transactions on Fuzzy Systems*, 2005, **13**(1): 1−12

21 Consolo G, Finocchio G, Carpentieri M, Cardelli E, Azzerboni B. About identification of scalar Preisach functions of soft magnetic materials. *IEEE Transactions on Magnetics*, 2006, **42**(4): 923−926

22 Ionita V, Cazacu E. Identification of hysteresis Preisach model using magneto-optic microscopy. *Physica B: Condensed Matter*, 2008, **403**(2-3): 376−378

23 Zhang H B, Jiang C B, Wang Z B, Xu H B. Effect of compressive stress on magnetostriction hysteresis of <110) oriented $Tb_{0.29}Dy_{0.48}Ho_{0.23}Fe_2$ crystal. *Journal of Alloys and Compounds*, 2009, **475**(1-2): 35−37

24 Venkataraman R, Krishnaprasad P S. Approximate inversion of hysteresis: theory and numerical results. In: Proceedings of the 39th IEEE Conference on Decision and Control. Sydney, Australia: IEEE, 2000. 4448−4454

25 Iyer R V, Tan X B. Control of hysteretic systems through inverse compensation. *IEEE Control Systems Magazine*, 2009, **29**(1): 83−99

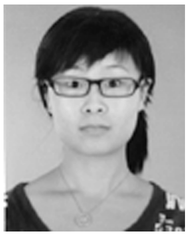

MA Yan-Hua Ph. D. candidate at the School of Automation Science and Electrical Engineering, Beihang University. She received her bachelor degree from Dalian University of Technology in 2004. Her research interest covers modeling and control of generalized dynamic hysteresis. Corresponding author of this paper.
E-mail: yh_ma@126.com

MAO Jian-Qin Professor at the School of Automation Science and Electrical Engineering, Beihang University. She received her Ph. D. degree from Beihang University in 1985. Her research interest covers fuzzy modeling and control with applications, and smart structure dynamics and control. E-mail: jqmao@buaa.edu.cn